analytical chemistry

Article

pubs.acs.org/ac

Dynamics of Conformational Ca^{2+}-Switches in Signaling Networks Detected by a Planar Plasmonic Device

Daniele Dell'Orco,*[,†,‡] Stefan Sulmann,[†] Sara Linse,[§] and Karl-Wilhelm Koch*[,†]

[†]Institute of Biology and Environmental Sciences, Biochemistry Group, University of Oldenburg, Carl-von-Ossietzky-Straße 9-11, D-26111 Oldenburg, Germany

[‡]Department of Life Sciences and Reproduction, Section of Biological Chemistry, University of Verona, Strada le Grazie 8, 37143 Verona, Italy

[§]Department of Biochemistry, Centre for Molecular Protein Science, Chemical Centre, Lund University, P.O. Box 124, SE-22100 Lund, Sweden

Supporting Information

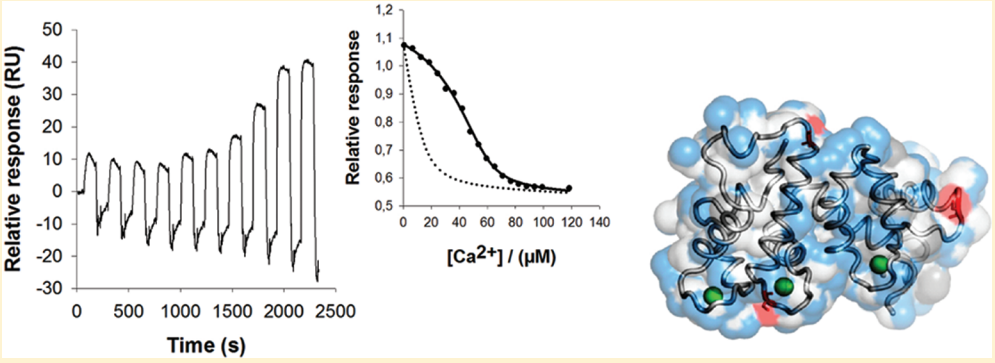

ABSTRACT: Ca^{2+}-sensor proteins regulate a variety of intracellular processes by adopting specific conformations in response to finely tuned changes in Ca^{2+}-concentration. Here we present a surface plasmon resonance (SPR)-based approach, which allows for simultaneous detection of conformational dynamics of four Ca^{2+}-sensor proteins (calmodulin, recoverin, GCAP1, and GCAP2) operating in the vertebrate phototransduction cascade, over variations in Ca^{2+} concentration in the 0.1−0.6 μM range. By working at conditions that quantitatively mimic those found in the cell, we show that the method is able to detect subtle differences in the dynamics of each Ca^{2+}-sensor, which appear to be influenced by the presence of free Mg^{2+} at physiological concentration and by posttranslational modifications such as myristoylation. Comparison between the macroscopic Ca^{2+}-binding constants, directly measured by competition with a chromophoric chelator, and the concerted binding-conformational switch detected by SPR at equilibrium reveals the relative contribution of the conformational change process to the SPR signal. This process appears to be influenced by the presence of other cations that perturb Ca^{2+}-binding and the conformational transition by competing with Ca^{2+}, or by pure electrostatic screening. In conclusion, the approach described here allows a comparative analysis of protein conformational changes occurring under physiologically relevant molecular crowding conditions in ultrathin biosensor layers.

Proteins are highly flexible macromolecules that adopt dynamic conformations depending on their sequence and conditions that underlie biological function.[1] A particularly interesting and ubiquitous class of proteins is that of Ca^{2+}-sensor proteins, which bind a well-defined number of Ca^{2+}-ions and switch between different conformations, often as a consequence of changes in intracellular Ca^{2+} triggered by physiological stimuli. In neurons, intracellular Ca^{2+} signals have crucial roles in activating neurotransmitter release and in triggering alterations in neuronal function.[2] An example of a finely Ca^{2+}-regulated signaling cascade is phototransduction in vertebrate rod cells, in which at least four Ca^{2+} sensors, namely, recoverin (Rec), calmodulin (CaM), and guanylate cyclase-activating proteins (GCAP1 and GCAP2) act simultaneously to regulate their targets as Ca^{2+} drops upon illumination from approximately 0.6 to 0.1 μM.[3] Physico-chemical methods that directly detect the conformational dynamics of Ca^{2+}-sensors are essential in order to elucidate at a systems-level the subtle differences in Ca^{2+} sensitivity constituting the regulatory basis of these complex networks.[4] Such methods would nonetheless be of little use, if the detection occurred in conditions very far from those within cells.

In the last years, the principle of surface plasmon resonance (SPR) has been widely used to study biomolecular interactions

Received: January 20, 2012
Accepted: February 27, 2012
Published: February 27, 2012

   dx.doi.org/10.1021/ac300213j | *Anal. Chem.* 2012, 84, 2982−2989

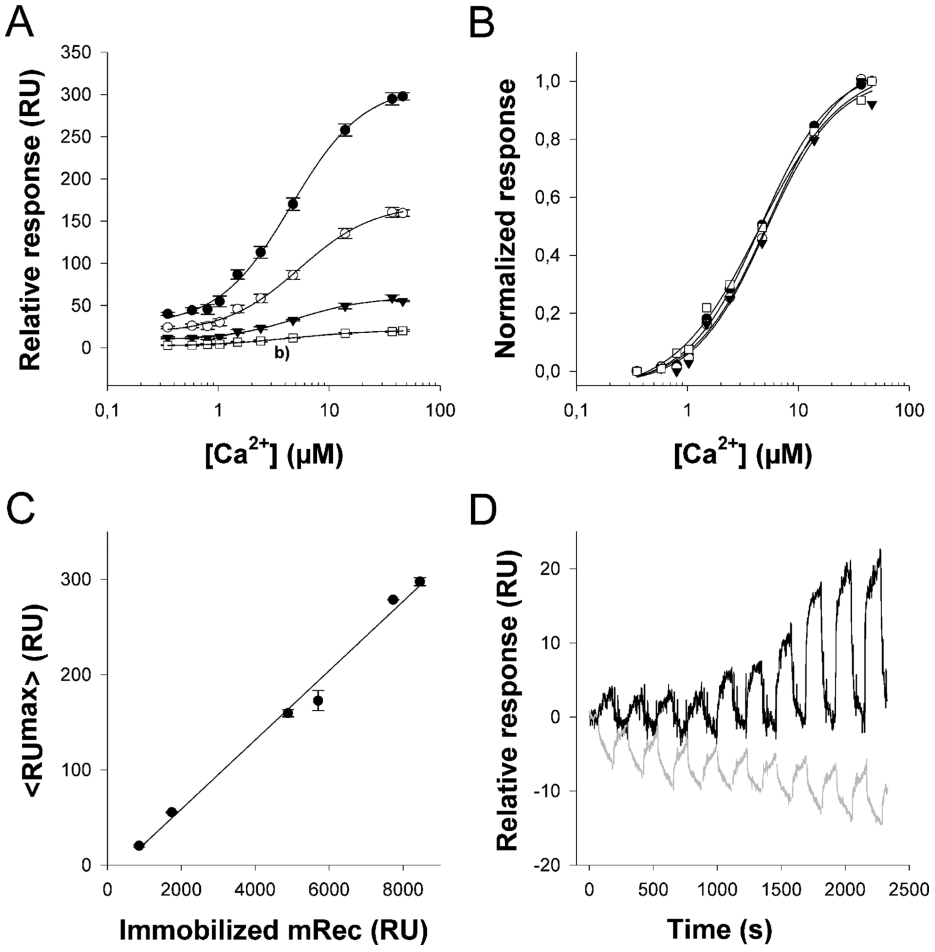

Figure 1. Effect of protein concentration and volumetric distribution on SPR detection of conformational changes in mRec at T = 25 °C. In each plot, error bars represent the SD (A) Different amounts of mRec ((●) 8453 RU, (○) 4885 RU, (▼) 1740 RU; (□) 860 RU) were immobilized on a 100 nm carboxymethyldextran-coated sensorchip and titrated with increasing Ca^{2+} concentration in the 0.3−46 μM range. Titrations were repeated three times (n = 3) and data were fitted according to a Hill-sigmoidal. (B) Normalized titration data. (C) Averaged maximal response upon titration plotted against the amount of immobilized mRec. The additional data points are from other immobilizations, including the one from ref.[13] The correlation coefficient is R^2 = 0.99. (D) Example of sensorgram obtained in Ca^{2+} titrations of mRec with 860 RU mRec immobilized on a 100 nm caboxymethyldextran-coated sensorchip (black trace) and the same amount immobilized on a flat carboxylated gold surface (gray trace).

and in a limited variety of cases also to detect protein conformational changes.[5−8] However, it should be pointed out that the working conditions were often far from physiological ones, especially in terms of protein and cofactor concentrations. In a number of cases, this led to potential artifacts likely due to the pH or salt effect on the matrix layers in which the proteins were embedded, with direct consequences on the refractive index changes hindering the real contribution of protein conformational change.[8,9] In order to avoid the drawbacks of SPR devices based on planar metal films, localized SPR (LSPR) nanodevices were recently developed.[10] Nanoparticles have been successfully used to enhance the SPR phenomenon at the nanoscale and found capable of detecting reversible Ca^{2+}-induced conformational changes in CaM-cutinase complex.[11,12] In a very recent work we determined the conditions under which widely available SPR instruments can be used to detect the conformational changes induced by Ca^{2+} binding to myristoylated (m)Rec with high accuracy and reproducibility.[13] mRec was immobilized on a carboxy-methyl-dextran (CMD) layer present on the surface of a commercial sensor chip via site-specific thiol-disulfide exchange.[13] Repeated pulses of Ca^{2+} in the physiological range induced reversible conformational changes in mRec, which were clearly detectable by an increase of the SPR signal far above the theoretical Ca^{2+}-binding capacity of the protein-coated surface, while substantially no response was observed for a mutant of mRec with impaired Ca^{2+}-binding capabilities.[13] Conformational transitions were reversed by switching from the Ca^{2+} injections to a decalcified buffer. Quantitative estimates of the equilibrium constant and the kinetic rate constants of the observed conformational transitions were consistent with each other, suggesting that the approach is also suitable to follow the time-course of the switches.

An essential feature of the above-mentioned approach is that the conformational change was studied under cellular-like conditions: mRec was immobilized at high density in the dextran matrix coating the sensor surface thereby reaching the micromolar concentration of mRec found in rod cells. Further, dextran itself is used as crowding agent in experimental approaches to simulate the macromolecular crowding conditions in cells.[14,15] In the present work we set out to investigate the general applicability of such method. In particular we sought to compare differences in Ca^{2+}-sensor dynamics within a specific signaling network, namely, the vertebrate phototransduction cascade. This system is well suited for investigating different conformational changes taking

dx.doi.org/10.1021/ac300213j | Anal. Chem. 2012, 84, 2982−2989

place in the same protein class. Mammalian photoreceptor cells house at least four Ca^{2+}-sensor proteins (cf. above) with distinct sensory and regulatory properties as they differ remarkably in their conformational changes triggered by Ca^{2+} binding or release, their dependence on other cations like Mg^{2+} and posttranslational modifications like myristoyl moieties.[16−18] For example, mRec undergoes a so-called Ca^{2+}-myristoyl switch by which the myristoyl group becomes expelled from the hydrophobic core of the protein upon Ca^{2+} binding. GCAP1 and 2 respond differently to Ca^{2+} binding with a smaller conformational arrangement around the myristoyl group. CaM on the other hand is not myristoylated, but exhibits distinct conformational shapes in its Ca^{2+}-bound and -free forms. These features allowed us to test for subtle differences in protein conformations under conditions of macromolecular crowding using a planar plasmonic device.

Finally, by comparing the binding equilibrium with the conformational equilibrium assessed by SPR, we could assess the relative contribution of the conformational change process to the observed signal.

EXPERIMENTAL SECTION

Protein Expression and Purification. Proteins were heterologuously expressed in *E. coli* and purified by size-exclusion chromatography and/or anion-exchange chromatography as reported (ref 18 for mRec, ref 19 for CaM^{S17C}, and refs 20 and 21 for GCAP1 and GCAP2 wild type and mutated forms). The purity of the obtained samples was verified by SDS-PAGE (see Supporting Information Figure S1). All proteins were dialyzed against decalcified NH_4HCO_3 buffer, concentrated, lyophilized and stored at −80 °C until use.

Ca^{2+}-Binding Assays with Chromophoric Chelator and Data Analysis. Ca^{2+}-titration experiments were performed as described,[22] by mixing similar concentrations (10−30 μM) of each protein and 5,5′Br_2-BAPTA chelator in decalcified buffer (5 mM Tris-HCl pH 7.5, 150 mM KCl). The absorbance at 263 nm (A_{263}) was monitored upon subsequent additions of 1−2 μL aliquots of 3 mM $CaCl_2$ until and beyond no change was observed. Initial protein concentrations were measured both by absorbance at 280 nm and by Coomassie blue dye assay,[23] yielding very similar results. The molar extinction coefficient used in the first case were 32 200 M^{-1} cm^{-1} for mRec,[18] 28 378 M^{-1} cm^{-1} for GCAP1,[24] 37 512 M^{-1} cm^{-1} for GCAP2,[24] and 2560 M^{-1} cm^{-1} for CaM (theoretically estimated from the amino acid composition). Further details are given in the Supporting Information. Initial Ca^{2+}-concentrations were found to range between 0.4 and 1 μM. Data were fitted with the CaLigator software[25] as elucidated elsewhere.[22] Each titration was repeated at least three times, both in the absence and in the presence of 1 mM Mg^{2+}, and the SD for each macroscopic binding constant was calculated based on the replicates.

SPR Experiments. SPR Ca^{2+}-titration experiments were performed as described[13] and specifically elucidated in Supporting Information.

RESULTS AND DISCUSSION

SPR-Based Detection of Conformational Dynamics Is Independent of the Amount of Immobilized Protein but Depends on the Sensing Volume. To allow for comparisons between proteins that show only slightly different Ca^{2+} affinities, the proposed methodology should be mostly independent of specific experimental settings. We thus asked whether the immobilization level of the protein on the sensor chip surface could potentially affect the detected dynamics. Different amounts of mRec (approximately 1 to 10 ng/flow cell, corresponding to 860−8450 RU; 1 RU = 1 pg/mm^2; flow cell area = 1.2 mm^2) were thus immobilized site-specifically via the unique Cys39 (numbering starts from the Met in the unprocessed protein) residue on a CMD-coated sensor chip, and subjected to ten injections of buffer with increasing Ca^{2+} concentration in the 0.3−46 μM range. Results of repeated injections and analysis of the maximum SPR amplitudes obtained upon each injection are reported in Figure 1A. Reducing the amount of immobilized protein merely resulted in an overall decrease of the observed SPR signal, while the shape of the curves remained the same, which is seen by overlapping the normalized curves as reported in Figure 1B. Moreover, when the data obtained in the present study are analyzed together with data obtained under the same conditions in our previous work,[13] a striking linear correlation is found between the maximum amplitude observed in Ca^{2+} titrations of mRec and the level of mRec immobilized (Figure 1C, R^2 = 0.99). Overall, these data suggest that increasing the amount of immobilized protein in the range 1−10 ng/flow cell leads to better signal-to-noise ratio without perturbing the observed dynamics. In order to assess whether the volumetric distribution of the protein within the volume of the flow cell had any effect on the intensity of the detected signal, we performed a control experiment with a sensor chip lacking the CMD-matrix. About 1 ng/flow cell (or 860 RU) of mRec was immobilized on the flat carboxylated surface using the same coupling chemistry as above. When subjected to identical injections of 0.3−46 μM Ca^{2+}, the two sensor chips showed a significantly different behavior (Figure 1D). When mRec was immobilized within the whole volume of the dextran matrix (∼100 nm thick layer) a reproducible and typical signal was detected in response to Ca^{2+} pulses (Figure 1D, black trace). In contrast, in the case of mRec adsorbed on a two-dimensional surface, Ca^{2+} injections led to a monotonic sequence of signals overlaying a rapid drift of the baseline that is most likely due to fast protein loss and degradation (Figure 1D, gray track). Hence, we conclude that the detection principle in our SPR-based approach relies on the whole volume of the flow cell, further confirming our prior interpretation that the detection of subtle conformational changes reflects changes in the whole dielectric milieu, including solvent rearrangement around immobilized proteins.[13]

Comparison of Direct Ca^{2+}-Binding and Induced Conformational Changes in Site-Specifically Immobilized Ca^{2+}-Sensors. We previously showed that in comparison with heterogeneous amine coupling, homogeneous immobilization via site specific thiol-coupling lead to remarkably cleaner single exponential binding processes for protein assembly[26] and to enhanced SPR signal upon metal ion binding to mRec.[13] Thus, in this study we sought to use the same coupling strategy to immobilize other phototransduction-related Ca^{2+} sensors on CMD-coated chips. While bovine mRec has a unique Cys at position 39, bovine CaM and mGCAP2 have either none or three Cys residues at positions 35, 111, and 131. Therefore we employed specific single-Cys mutants of both proteins, namely CaM^{S17C} and $mGCAP2^{CAA}$, which were previously designed (ref 19 and ref 27, respectively).

A comparative test of Ca^{2+}-induced conformational changes in these three Ca^{2+} sensors as monitored by SPR is given in

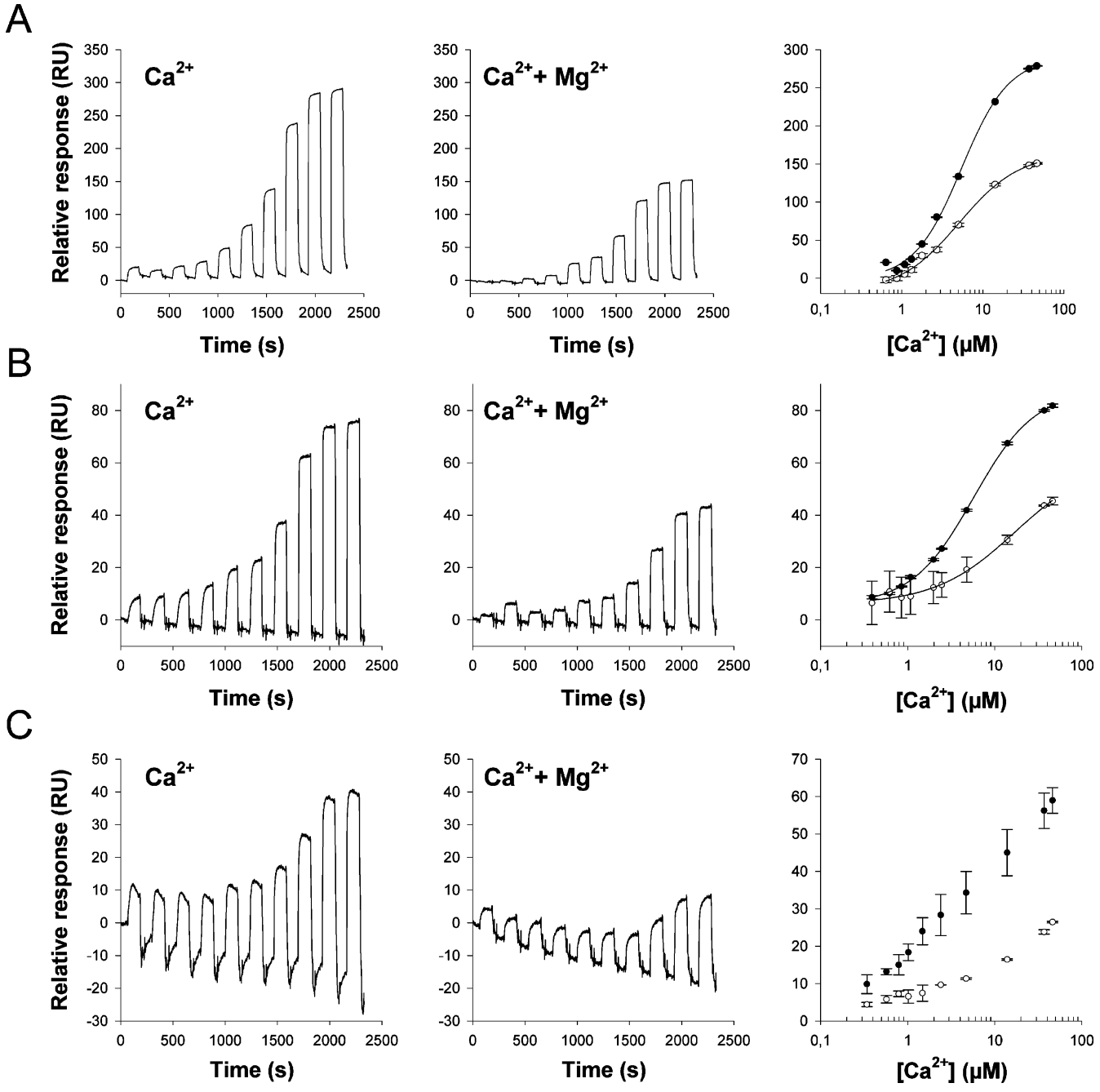

Figure 2. SPR detection of conformational changes in three different Ca^{2+} sensors site-specifically coupled to the surface, at T = 25 °C. Examples of sensorgrams obtained upon Ca^{2+}-titrations in the absence (left panel) and presence of 1 mM free Mg^{2+} (middle panel) are reported, together with the plot of the maximal amplitude as a function of Ca^{2+} (right panel; the error bars represent the SD; (●) without Mg^{2+}, (○) with 1 mM free Mg^{2+}). (A) Example of a sensorgram obtained for mRec. Data fitting by a Hill sigmoidal curve resulted in $K_{1/2}^{SPR}$=5.5 ± 0.1 μM for the Ca^{2+}-titration (n = 2) and a $K_{1/2}^{SPR}$=5.2 ± 0.1 μM (n = 4) in the presence of 1 mM Mg^{2+}. (B) Example of a sensorgram obtained for CaM^{S17C}. Data fitting by a Hill sigmoidal curve resulted in $K_{1/2}^{SPR}$=5.70 ± 0.03 μM for the Ca^{2+}-titration (n = 4) and a $K_{1/2}^{SPR}$=17.2 ± 0.4 μM (n = 3) in the presence of 1 mM Mg^{2+}. (C) Example of a sensorgram obtained for $mGCAP2^{CAA}$. The titration did not lead to complete saturation and the data could not be fitted by the same model.

Figure 2. Titrations of immobilized mRec and CaM^{S17C} revealed similar overall spiking patterns (Figures 2A and B), only the amplitudes were lower in the case of CaM^{S17C}. It is also worth noting that the immobilized amount of CaM^{S17C} (8.2 ng/flow cell) and mRec (9.3 ng/flow cell) differed approximately by 10%, but the maximal amplitudes of the detected conformational changes were much lower for CaM^{S17C} (~80 RU) compared to mRec (~300 RU). This could reflect, at least in part, the significantly different change in solvent accessible surface area (SAS) of the two sensors upon Ca^{2+}-binding. While mRec switches from a 10 333 Å^2 (apo) to a 12 014 Å^2 SAS upon Ca^{2+}-binding,[13] the change is significantly smaller in CaM (9684 Å^2 for the apo form, versus 9721 Å^2 for the Ca^{2+}-bound form in the typical dumbbell shape; values were computed by comparing the three-dimensional structures of the two proteins, PDB entries 1DMO[28] and 1CLL,[29] respectively).

The main effect observed in the presence of 1 mM Mg^{2+} was a reduction of the amplitudes reached upon each Ca^{2+}-

dx.doi.org/10.1021/ac300213j | Anal. Chem. 2012, 84, 2982−2989

Table 1. Results of Ca^{2+}-Binding Experiments and SPR-Based Detection of Conformational Changes[a]

		log K_1	log K_2	log K_3	log K_4	K_D^{app} (μM)	$K_{1/2}^{SPR}$ (μM)	K_{cc}
CaM^{S17C}	Ca^{2+}	5.6 ± 0.5	5.9 ± 0.6	(4.7 ± 0.6)	6.0 ± 0.6	1.6	5.7 ± 0.03	2.8×10^{-1}
	Ca^{2+} + Mg^{2+}	5.6 ± 0.2	5.3 ± 0.5	5.3 ± 0.4	(4.4 ± 1)	4.0	17.2 ± 0.4	2.3×10^{-1}
mGCAP2	Ca^{2+}	6.9 ± 0.7	(4.9 ± 0.3)	7.3 ± 0.8		0.08	24.9 ± 0.2	3.2×10^{-3}
	Ca^{2+} + Mg^{2+}	6.7 ± 0.1	5.9 ± 0.3	5.2 ± 0.2		0.50	37.7 ± 0.5	1.3×10^{-2}
$mGCAP2^{CAA}$	Ca^{2+}	6.6 ± 0.3	6.4 ± 0.2	5.6 ± 0.3		0.32	ND	ND
	Ca^{2+} + Mg^{2+}	6.7 ± 0.5	6.3 ± 0.6	(4.8 ± 0.4)		0.32	ND	ND
$mGCAP1^{D6S}$	Ca^{2+}	7.1 ± 0.9	6.5 ± 0.8	6.1 ± 0.5		0.16	19.7 ± 0.8	8.1×10^{-3}
	Ca^{2+} + Mg^{2+}	6.7 ± 0.8	5.9 ± 0.1	6.1 ± 1.0		0.50	25.4 ± 1.2	2.0×10^{-2}
$nmGCAP1^{CAAA}$	Ca^{2+}	7.4 ± 0.2	6.1 ± 0.5	6.5 ± 0.8		0.16	ND	ND
	Ca^{2+} + Mg^{2+}	7.1 ± 0.4	6.0 ± 0.5	6.4 ± 0.5		0.25	ND	ND

[a]Decimal logarithm of each macroscopic binding constant as obtained from fitting performed with the software Caligator.[25] Errors represent SD of repeated determinations. K_D^{app} represent the apparent affinity as obtained from averaging the significant macroscopic binding constants. $K_{1/2}^{SPR}$ was obtained by fitting by a Hill sigmoidal the average maximum amplitudes upon Ca^{2+}-injection as a function of free-Ca^{2+} in SPR experiments. K_{cc} was obtained from eq 1.

injection, which in the case of mRec rendered the transitions almost undetectable for the first injections at lower Ca^{2+} concentration (Figure 2A, middle and right panels). The high reproducibility and the level of saturation allowed us to estimate $K_{1/2}^{SPR}$, which is defined as the Ca^{2+} concentration at which the signal change due to the conformational transition was half-maximal (Figure 2A and B, right panel). Interestingly, no significant difference in $K_{1/2}^{SPR}$ was observed for mRec in the presence or absence of 1 mM Mg^{2+}, that is, $K_{1/2}^{SPR}$=5.5 ± 0.1 μM and $K_{1/2}^{SPR}$=5.2 ± 0.1 μM, respectively. Moreover, a greater variability in the response was observed for CaM^{S17C} in the presence of 1 mM Mg^{2+} as highlighted by larger error bars (Figure 2B, right panel). Interestingly, and different from mRec, CaM^{S17C} showed a significant shift in $K_{1/2}^{SPR}$ values, from 5.70 μM to 17.2 μM respectively in the absence and in the presence of Mg^{2+} (Table 1), hence resulting in a ~3-fold increase.

To distinguish the effect of Ca^{2+} on triggering a conformational change from its direct binding to the Ca^{2+}-sensor proteins we also measured Ca^{2+}-binding by an established titration method based on the competition for Ca^{2+} between the protein and a chromophoric chelator.[22,25,30] Binding measurements were performed both in the absence and in the presence of 1 mM Mg^{2+}, corresponding to the physiological free levels found in rod cells. The macroscopic binding constants obtained in each case are reported, together with the apparent affinity K_D^{app} in Table 1, while examples of the titration curves are reported in Supporting Information Figure S1. Values of Ca^{2+}-binding to mRec have been studied extensively and were also compared in our previous study;[13] they are, therefore, not included here.

Good agreement was achieved between the values obtained in this study (Table 1) for the CaM^{S17C} macroscopic binding constants and those previously found for wild type CaM,[31] as reflected by the very similar K_D^{app} values (1.6 versus 1.8 μM, respectively). This confirms that the S17C substitution does not significantly perturb the Ca^{2+} binding to CaM. Experiments performed in the presence of 1 mM Mg^{2+} led to a significant reduction in Ca^{2+}-affinity for CaM^{S17C} (Table 1), resulting in a 4 μM K_D^{app}, hence a ~2.2-fold reduction.

Results were found to be significantly different for the $mGCAP2^{CAA}$ mutant. Direct Ca^{2+}-binding assay showed a significantly lower (4-fold) affinity in the absence of Mg^{2+} as compared to the wild type form (K_D^{app} = 0.32 μM versus 0.08 μM, respectively). Moreover, when the binding experiments were performed in the presence of 1 mM Mg^{2+} the wild type form showed a K_D^{app} of 0.50 μM, within the physiological range of free Ca^{2+}, while the CAA mutant showed substantially unaltered affinity (Table 1). This suggests that the mutations may have perturbed at least one of the three Ca^{2+}-binding sites. Moreover, this mutant displays biphasic SPR data (Figure 2C). In spite of the very high immobilization level obtained (14.5 ng/flow cell), the changes in response to Ca^{2+}-injections were significantly lower compared to other proteins (50 RU maximum), and the pattern was completely different. An initial rapid increase of the signal was followed by a slow decrease, a scheme that was symmetrically reversed upon Ca^{2+}-dissociation. Moreover, a continuous drift in the signal was observed, which reduced the overall reproducibility (Figure 2C, right panel). Although this behavior prevented data fitting, it is noteworthy that the presence of 1 mM Mg^{2+} significantly changed the observed pattern (Figure 2C, middle panel). While a reduction of the amplitudes was observed, the pattern of the injections appeared different and indicative of substantially slower processes.

The analysis was completed by SPR experiments performed with the wild type forms of mGCAP1 and mGCAP2. Considering that these forms have four and three Cys residues, respectively, we immobilized them via heterogeneous amine-coupling at high immobilization levels (10.8 ng/flow cell mGCAP1 and 8.2 ng/flow cell mGCAP2). Results of SPR-monitored Ca^{2+}-titrations are reported in Supporting Information Figures S2 and S3. Different patterns were observed and in spite of the significantly higher immobilization level, mGCAP1 showed slightly lower amplitudes in response to Ca^{2+}compared to mGCAP2 (compare Supporting Information Figures S2 and S3). Moreover, the same negative-positive zigzag variation upon Ca^{2+}-injection found for $mGCAP2^{CAA}$ was observed for the wild type form, but the initially fast increase of the signal was missing (Supporting Information Figure S2). Despite the drift present in both cases, the signals were fairly reproducible and reached in both cases saturation (Supporting Information Figures S2 and S3), which allowed determining $K_{1/2}^{SPR}$ values. Interestingly, the presence of 1 mM Mg^{2+} shifted such values to higher Ca^{2+} in both cases (Table 1). It is also worth noting that for mGCAP1 the presence of 1 mM Mg^{2+} tuned the equilibrium Ca^{2+}-dissociation constant to a value of 0.5 μM, hence fully compatible with the physiological working range of the sensor.

Taken together, the analysis of the equilibrium data obtained by SPR (Figure 2A–B and Supporting Information Figures S2

dx.doi.org/10.1021/ac300213j | Anal. Chem. 2012, 84, 2982–2989

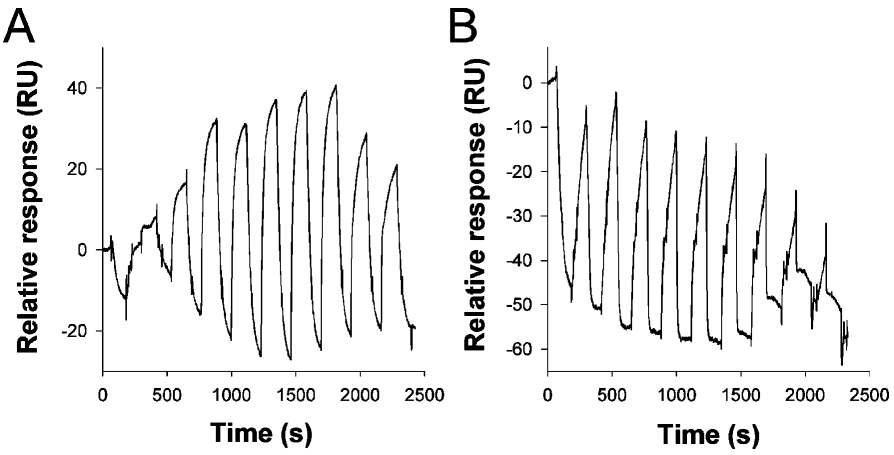

Figure 3. Example of SPR detection of conformational changes in nonmyristoylated Rec (approximately 6000 RU immobilized, (A)) and nonmyristoylated GCAP1^{CAAA} (approximately 12 000 RU immobilized, (B)) upon Ca^{2+}-titration at T = 25 °C.

and S3, right panels) and the Ca^{2+}-binding affinity directly measured by the chelator assay (Table 1) allows estimation of the conformational change contribution (K_{cc}) in the concerted binding-conformational transition process, from the relationship:

$$K_{tot} = \frac{1}{K_{1/2}^{SPR}} = \frac{K_{cc}}{K_D^{app}} \quad (1)$$

Values obtained for the unitless quantity K_{cc} are reported in Table 1, for cases in which saturation was clearly observed in SPR experiments and eq 1 could therefore be used.

For both mGCAP1 and mGCAP2 the K_{cc} values were significantly lower compared to CaM^{S17C} and comparable with each other (Table 1). In detail, a ∼4-fold higher K_{cc} was found for mGCAP2 in the presence of Mg^{2+}, while a lower effect (∼2.5-fold) was observed for mGCAP1. In both cases, however, Mg^{2+} clearly influenced the dynamics and the magnitude of the conformational changes. The relatively high K_{cc} values obtained for CaM^{S17C} as compared to those for GCAPs (Table 1), indicative of a major structural rearrangement, is paralleled by a very minor effect of Mg^{2+} on the energetics of conformational changes (0.28 vs 0.23 K_{cc}). A possible interpretation is that the remarkable shift observed in $K_{1/2}^{SPR}$ reflects the significant reduction of affinity for Ca^{2+} in the presence of physiological Mg^{2+}[32,33] rather than a different mechanism for the conformational transition. The reduction in apparent Ca^{2+} affinity is most marked for the N-terminal sites of CaM,[32] which have higher Mg^{2+} affinity than the C-terminal sites.

Effect of Myristoylation on the Conformational Dynamics of Rec and GCAP1. Myristoylation of Ca^{2+}-sensor proteins can modify their specific regulatory properties including activation of their targets. Moreover, it has been shown that although the overall architecture of the protein and the Ca^{2+}-binding domains is conserved, the acyl modification can affect the structure differently, depending on the of Ca^{2+}-sensor.[34−37] The structural effect because of the absence of myristoylation on GCAP1 resulted in significantly lowered thermal stabilities both in the apo and in the Ca^{2+}-bound form, despite the affinity for Ca^{2+} was only marginally affected.[22] To investigate directly the dynamics of Ca^{2+} binding to nonmyristoylated sensors, we produced a nonmyristoylated variant (nmGCAP1^{CAAA}) of GCAP1, in which the only residual Cys is the one at position 18,[21] and then we immobilized at high level both nmRec (7.2 ng/flow cell) and nmGCAP1^{CAAA} (14−16 ng/flow cell) via site-specific thiol coupling. Ca^{2+} pulses in the 0.3−46 μM range led to remarkably different patterns compared to all the other myristoylated proteins studied here (Figure 3). Relatively slow, nonsaturating kinetics with overall lower maximal amplitude compared to the myristoylated case were observed for nmRec (Figure 3A). The variation of the SPR signal upon Ca^{2+} injections showed an opposite trend as compared to mRec, in that it decreased upon injection/association and increased upon dissociation.

The kinetics at increasing Ca^{2+} did not differ substantially from each other, as confirmed by the very similar shapes in both phases, but the amplitude of the responses was higher for intermediate Ca^{2+}-concentrations in the 1−2.5 μM. The counterintuitive pattern was reproducible upon several repetitions. A different result was obtained for nmGCAP1^{CAAA}, (Figure 3B) for which increasing Ca^{2+} injections in the 0.3−1 μM range led to a significant acceleration of the association/transition kinetics, which appeared to saturate after the second injection (0.6 μM), in contrast to the dissociation/relaxation kinetics which appeared significantly slower the higher the Ca^{2+}-concentration of the injected sample (Figure 3B). The pattern was also completely different compared to that of mGCAP1, and as for nmRec it was characterized by negative signals upon Ca^{2+}-injections.

In agreement with structural information about nmRec in the literature,[38] we propose that the lack of myristoylation for nmGCAP1^{CAAA} might lead to a more flexible conformation. This would explain why, in both cases, overall lower maximal amplitude observed in the whole titration pattern is paralleled by significantly higher variations of the SPR response upon individual injections as compared to the respective myristoylated cases (Figure 2 and Supporting Information Figure S3). From these results, it appears clear that the method is able to detect with high sensitivity the effect of myristoylation on the conformational dynamics.

Influence of Specific Metal Cations on the Detected Conformational Dynamics. Depending on the specific protein, the presence of 1 mM Mg^{2+} was found to influence either the Ca^{2+} binding, the concerted conformational transition, or both (Table 1). To investigate the physicochemical nature of such effects, we immobilized mRec and followed by SPR the Ca^{2+}-titrations in the presence of other salts at

dx.doi.org/10.1021/ac300213j | Anal. Chem. 2012, 84, 2982−2989

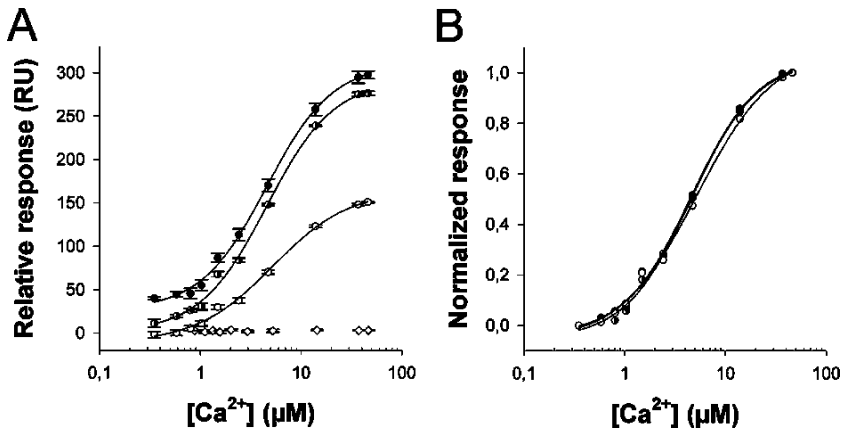

Figure 4. Effect of increased ionic strength on the SPR detection of conformational changes in mRec (T = 25 °C). (A) The Ca^{2+}-titration was repeated with the same immobilized sample in normal running buffer (●) (n = 2); in the presence of additional 2 mM K^+ (□) (n = 3); in the presence of 1 mM Mg^{2+} (○) (n = 4); in the presence of 1 mM Zn^{2+} (◊) (n = 3). Error bars stand for the SD (B) Normalization of the plots obtained in (A), except for the one referring to $ZnCl_2$.

concentrations yielding the same ionic strength as 1 mM Mg^{2+}. For this purpose, 2 mM KCl and 1 mM $ZnCl_2$ were added to the running buffer and to the Ca^{2+} stocks to be injected in SPR experiments. Results of Ca^{2+}-titrations in the 0.3−46 μM range are shown in Figure 4A. Interestingly, the addition of 2 mM K^+ reduced the amplitude of each individual response by approximately 8%, hence suggesting a pure electrostatic screening effect as the only consequence. NMR studies have in fact shown that weak binding of K^+ to CaM has only minimal structural effects.[31] A significantly higher reduction of the maximal amplitudes (~50%) was observed in the presence of 1 mM Mg^{2+}, as already discussed and shown (Figure 2A). However, neither of the added cations significantly shifted in the measured $K_{1/2}^{SPR}$ values, as the normalized data in Figure 4B clearly show.

A completely different behavior was observed when the titrations were performed in the presence of 1 mM Zn^{2+}. In this case, no change in the SPR signal was detected upon the same Ca^{2+} titrations (Figure 4A). This result is in line with the known Zn^{2+} affinity for mRec, with an apparent K_D of 30 μM for the apo-state.[39] The binding sites for Zn^{2+} are distinct from those of Ca^{2+}, and structural studies showed that Zn^{2+} binding causes the protein to expose hydrophobic residues, hence inducing their solvation.[39] The high concentration of Zn^{2+} in our SPR experiments thus ensures high saturation levels to apo mRec and may favor a conformation that is incompatible with the Ca^{2+}-switch clearly visible with all the other cations.

Monitoring Different Kinetics of the Conformational Dynamics of Ca^{2+}-Sensors Triggered by Physiological Ca^{2+}-Stimuli. A closer inspection of the SPR responses obtained during the Ca^{2+}-titrations revealed differences in the kinetics of response to Ca^{2+} (Figure 2 and Supporting Information Figures S2 and S3). These differences are highlighted in Figure 5. We triggered the Ca^{2+}-induced conformational change of four proteins (mRec, $mGCAP2^{CAA}$, CaM^{S17C}, $nmGCAP1^{CAAA}$) by injecting physiological concentrations of Ca^{2+}. While both the binding/switch and dissociation/relaxation were relatively fast for mRec (black trace) and $mGCAP2^{CAA}$ (green trace), a significantly slower binding/switch process was observed for CaM^{S17C} (blue trace), which however reversed very fast. The slowest processes were observed for $nmGCAP1^{CAAA}$ (red trace) at this Ca^{2+} level. We interpret these data as to reflect dielectric changes in the

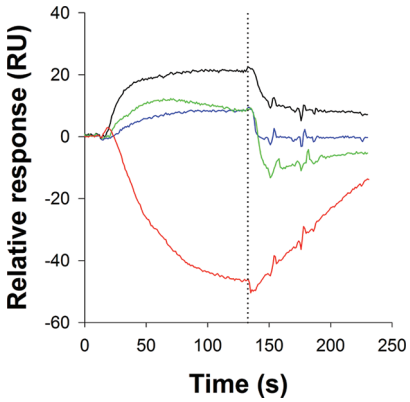

Figure 5. Comparison of the kinetics of conformational changes upon Ca^{2+}-binding of $nmGCAP1^{CAAA}$ (14.5 ng/flow cell immobilized; red line), $mGCAP2^{CAA}$ (14.5 ng/flow cell immobilized; green line), CaM^{S17C} (8.2 ng/flow cell immobilized; blue line), and mRec (9.3 ng/flow cell immobilized; black line) at T = 25 °C in the physiological range of Ca^{2+} (0.35, 0.35, 0.39, and 0.64 μM, respectively).

hydrodynamic vicinity of the proteins occurring at different velocities, which might ultimately originate from differences in concerted protein and solvent rearrangement dynamics. However, our current SPR approach has a too low time-resolution as to monitor dynamic changes in protein conformation on a nanosecond time scale. Therefore, it is limited to a qualitative conclusion and does not allow a detailed kinetic analysis. Although in cases where the Ca^{2+}-induced conformational transition occurs between particularly defined and stable states, such as for mRec, a kinetic analysis was possible and led to results consistent with those obtained by equilibrium analyses,[13] this does not appear to be a general condition for all the proteins tested here. Future work is intended to investigate this aspect.

CONCLUSIONS

A distinctive advantage of the SPR methodology presented here is that different Ca^{2+}-sensor proteins can be immobilized on the same sensor chip at concentrations that mimic those found in the cell, by exploiting the whole volumetric extension of the flow cell via the CMD matrix rather than the limited surface of the metal film. Considering that no other chemical is needed to

dx.doi.org/10.1021/ac300213j | Anal. Chem. 2012, 84, 2982−2989

reverse conformational changes, this provides a unique opportunity to follow in label-free conditions the simultaneous effects of the same Ca^{2+}-signal on different Ca^{2+}-sensors, hence highlighting specific differences in the conformational dynamics. This aspect is crucial to unraveling the dynamics of Ca^{2+}-regulated signaling networks at a systems-level.

■ ASSOCIATED CONTENT

Supporting Information

Complete experimental details and supplementary figures (Figure S1, Figure S2, and Figure S3). This material is available free of charge via the Internet at http://pubs.acs.org.

■ AUTHOR INFORMATION

Corresponding Author

*Telephone: +39-045-802-7637 (D.D.); +49-(0)441-798-3640 (K.-W.K). E-mail: daniele.dellorco@univr.it (D.D.); karl.w.koch@uni-oldenburg.de (K.-W.K).

Notes

The authors declare no competing financial interest.

■ ACKNOWLEDGMENTS

This work was funded by an A. von Humboldt Fellowship and a Fellowship from the Hanse-Wissenschaftskolleg Delmenhorst, Germany to DDO, by a grant from the DFG to KWK (KO 948/10-1) and by a grant from the Crafoord Foundation to SL.

■ REFERENCES

(1) Henzler-Wildman, K.; Kern, D. *Nature* **2007**, *450*, 964−972.
(2) Burgoyne, R. D. *Nat. Rev. Neurosci.* **2007**, *8*, 182−193.
(3) Pugh, E. N., Jr..; Lamb, T. D. *Phototransduction in Vertebrate Rods and Cones: Molecular Mechanisms of Amplification, Recovery and Light Adaptation*; Elsevier Science B.V: Amsterdam, 2000.
(4) Dell'Orco, D.; Schmidt, H.; Mariani, S.; Fanelli, F. *Mol. Biosyst.* **2009**, *5*, 1232−1246.
(5) Christopeit, T.; Gossas, T.; Danielson, U. H. *Anal. Biochem.* **2009**, *391*, 39−44.
(6) Gestwicki, J. E.; Hsieh, H. V.; Pitner, J. B. *Anal. Chem.* **2001**, *73*, 5732−5737.
(7) Sota, H.; Hasegawa, Y.; Iwakura, M. *Anal. Chem.* **1998**, *70*, 2019−2024.
(8) Winzor, D. J. *Anal. Biochem.* **2003**, *318*, 1−12.
(9) Paynter, S.; Russell, D. A. *Anal. Biochem.* **2002**, *309*, 85−95.
(10) Haes, A. J.; Van Duyne, R. P. *Anal. Bioanal. Chem.* **2004**, *379*, 920−930.
(11) Hall, W. P.; Anker, J. N.; Lin, Y.; Modica, J.; Mrksich, M.; Van Duyne, R. P. *J. Am. Chem. Soc.* **2008**, *130*, 5836−5837.
(12) Hall, W. P.; Modica, J.; Anker, J.; Lin, Y.; Mrksich, M.; Van Duyne, R. P. *Nano Lett* **2011**, *11*, 1098−1105.
(13) Dell'Orco, D.; Muller, M.; Koch, K. W. *Chem Commun (Cambridge, U.K.)* **2010**, *46*, 7316−7318.
(14) Ghahghaei, A.; Rekas, A.; Price, W. E.; Carver, J. A. *Biochim. Biophys. Acta* **2007**, *1774*, 102−111.
(15) Zimmerman, S. B.; Minton, A. P. *Annu. Rev. Biophys. Biomol. Struct.* **1993**, *22*, 27−65.
(16) Peshenko, I. V.; Dizhoor, A. M. *J. Biol. Chem.* **2006**, *281*, 23830−23841.
(17) Peshenko, I. V.; Dizhoor, A. M. *J. Biol. Chem.* **2007**, *282*, 21645−21652.
(18) Senin, I. I.; Fischer, T.; Komolov, K. E.; Zinchenko, D. V.; Philippov, P. P.; Koch, K. W. *J. Biol. Chem.* **2002**, *277*, 50365−50372.
(19) O'Connell, D. J.; Bauer, M. C.; O'Brien, J.; Johnson, W. M.; Divizio, C. A.; O'Kane, S. L.; Berggard, T.; Merino, A.; Akerfeldt, K. S.; Linse, S.; Cahill, D. J. *Mol. Cell Proteomics* **2010**, *9*, 1118−1132.
(20) Helten, A.; Saftel, W.; Koch, K. W. *J. Neurochem.* **2007**, *103*, 1439−1446.
(21) Hwang, J. Y.; Schlesinger, R.; Koch, K. W. *FEBS Lett.* **2001**, *508*, 355−359.
(22) Dell'Orco, D.; Behnen, P.; Linse, S.; Koch, K. W. *Cell. Mol. Life Sci.* **2010**, *67*, 973−984.
(23) Bradford, M. M. *Anal. Biochem.* **1976**, *72*, 248−254.
(24) Hwang, J. Y.; Lange, C.; Helten, A.; Hoppner-Heitmann, D.; Duda, T.; Sharma, R. K.; Koch, K. W. *Eur. J. Biochem.* **2003**, *270*, 3814−3821.
(25) Andre, I.; Linse, S. *Anal. Biochem.* **2002**, *305*, 195−205.
(26) Dell'Orco, D.; Xue, W. F.; Thulin, E.; Linse, S. *Biophys. J.* **2005**, *88*, 1991−2002.
(27) Helten, A.; Koch, K. W. *Biochem. Biophys. Res. Commun.* **2007**, *356*, 687−692.
(28) Zhang, M.; Tanaka, T.; Ikura, M. *Nat. Struct. Biol.* **1995**, *2*, 758−767.
(29) Chattopadhyaya, R.; Meador, W. E.; Means, A. R.; Quiocho, F. A. *J. Mol. Biol.* **1992**, *228*, 1177−1192.
(30) Linse, S. In *Calcium-Binding Protein Protocols: Vol. 2: Methods and Techniques*; Vogel, H. J., Ed.; Humana Press: Calgary, Canada, 2002; Vol. *173*, pp 15−24.
(31) Linse, S.; Helmersson, A.; Forsen, S. *J. Biol. Chem.* **1991**, *266*, 8050−8054.
(32) Malmendal, A.; Linse, S.; Evenas, J.; Forsen, S.; Drakenberg, T. *Biochemistry* **1999**, *38*, 11844−11850.
(33) Martin, S. R.; Masino, L.; Bayley, P. M. *Protein Sci.* **2000**, *9*, 2477−2488.
(34) Ames, J. B.; Dizhoor, A. M.; Ikura, M.; Palczewski, K.; Stryer, L. *J. Biol. Chem.* **1999**, *274*, 19329−19337.
(35) Ames, J. B.; Ishima, R.; Tanaka, T.; Gordon, J. I.; Stryer, L.; Ikura, M. *Nature* **1997**, *389*, 198−202.
(36) Stephen, R.; Bereta, G.; Golczak, M.; Palczewski, K.; Sousa, M. C. *Structure* **2007**, *15*, 1392−1402.
(37) Tanaka, T.; Ames, J. B.; Harvey, T. S.; Stryer, L.; Ikura, M. *Nature* **1995**, *376*, 444−447.
(38) Flaherty, K. M.; Zozulya, S.; Stryer, L.; McKay, D. B. *Cell* **1993**, *75*, 709−716.
(39) Permyakov, S. E.; Cherskaya, A. M.; Wasserman, L. A.; Khokhlova, T. I.; Senin, I. I.; Zargarov, A. A.; Zinchenko, D. V.; Zernii, E. Y.; Lipkin, V. M.; Philippov, P. P.; Uversky, V. N.; Permyakov, E. A. *J Proteome Res* **2003**, *2*, 51−57.